EUROPEAN JOURNAL OF COMPUTATIONAL MECHANICS, 2015
VOL. 24, NO. 6, 279–301
http://dx.doi.org/10.1080/17797179.2016.1181031

Taylor & Francis
Taylor & Francis Group

MHD Stokes flow in lid-driven cavity and backward-facing step channel

Merve Gürbüz and M. Tezer-Sezgin

Department of Mathematics, Middle East Technical University, Ankara, Turkey

ABSTRACT

The 2D Magnetohydrodynamics Stokes flow equations are solved in a lid-driven cavity and backward-facing step channel in the presence of a uniform magnetic field with different orientations. The hydrodynamic and electromagnetic equations are solved simultaneously using Stokes approximation in terms of velocity, pressure, stream function and vorticity with an iterative procedure. The radial basis function approximations are used to terms other than diffusion satisfying the boundary conditions at the same time, and obtaining not only the particular solution but the solution itself. It is found that as the strength of the applied magnetic field increases, boundary layers are formed close to the moving lid and in the separation region of main and secondary flows in the lid-driven cavity. In the step flow, an increase in Hartmann number causes the enlargement of recirculation flow in front of the step and the fully developed flow after the step when magnetic field applies horizontally, whereas *y*-direction magnetic field helps to diminish this recirculation. Pressure increases in the channel with increasing magnetic effect. The solution is obtained easily in a considerably low-computational cost through the use of radial basis function approximation.

ARTICLE HISTORY
Received 27 October 2015
Accepted 18 April 2016

KEYWORDS
MHD Stokes flow; electric potential; RBF approximation; lid-driven cavity; backward-facing step flow

1. Introduction

Magnetohydrodynamics (MHD) is the branch of fluid mechanics that focuses on the flow of electrically conducting fluids in the presence of magnetic field. Its popularity comes from the wide range of industrial applications such as MHD pumps, geothermal energy extraction, liquid metal productions (mercury, liquid sodium, etc.), plasma physics and nuclear fusion. The MHD equations are modelled by the coupled physical systems through Ohm's law as the motion of Newtonian fluids governed by the Navier–Stokes equations and the electromagnetic effects governed by Maxwell's equations. A number of physical assumptions valid for the problem of interest such as small Reynolds number (Re) and/or small magnetic Reynolds number (R_m) reduce these two systems to the final MHD equations considered. In this study, both Re and R_m are assumed to be small which result in slow flow (Stokes approximation) and negligible induced magnetic field in the

CONTACT M. Tezer-Sezgin munt@metu.edu.tr

fluid, that is going to be termed as MHD Stokes flow. (These flows refer to fluid motions that are dominated by viscosity and the flow is slow, creeping.)

Stokes flow has been studied by several numerical approaches. Smyrlis and Karageorghis (2003) have transformed 2D Stokes equations into the biharmonic equation using the stream function formulation and solved with the method of fundamental solutions (MFS). Tsai, Young, and Cheng (2002) applied MFS to 3D Stokes flow in velocity–vorticity formulation. Numerical results for 2D Stokes flow in cavities have been carried out by Alves and Silvestre (2004), Young, Chen, Fan, Murugesan, and Tsai (2005) and Chen et al. (2005) using MFS. Young, Jane, Fan, Murugesan, and Tsai (2006) extended MFS solution to 2D irregular geometry and 3D Stokes flows in terms of all field variables. In these studies, the effects of number of source points in MFS and their locations on the numerical accuracy have been discussed. Fan and Young (2002), Young, Jane, Lin, Chiu, and Chen (2004) have also considered solutions of Stokes flow by boundary integral equation method and multiquadratic method, respectively.

In the above studies, either biharmonic stream function or velocity–vorticity Poisson's equations or velocity–pressure–stream function formulations have been taken to solve Stokes flow. The fluid motion is considered only under the effect of pressure gradient and gravitational force where applicable. It is important to simulate the behaviours of velocity components separately, and the flow field in terms of streamlines as well as the pressure and vorticity behaviours especially when an external magnetic field is present which changes the profile of the flow field considerably. Thus, in this work, MHD Stokes flow equations are presented containing all the flow field variables as velocity, pressure, stream function and vorticity to demonstrate the changes with respect to several values of Hartmann number including strength of applied magnetic field.

In this study, the radial basis function (RBF) approximation has been used to solve 2D MHD Stokes flow equations in a lid-driven rectangular cavity and over a backward-facing step with different configurations of the externally applied magnetic field. RBF approximation has been applied by Kutanaei et al. (2012) for solving Stokes flow in a circular cavity using mesh-free local RBF-DQ method, Bustamante, Power, Sua, and Florez (2013) carried integrated RBF method for solving Stokes flow in cavities and over backward-facing step by taking multiquadratic RBFs. Kefayati, Gorji-Bandpy, Sajjadi, and Ganji (2012) have solved MHD mixed convection in a lid-driven cavity for linearly heated wall using lattice Boltzmann method. Results are given for several values of Hartmann number, Richardson number for $Re = 100$ in the case of external magnetic field applied in x- and/or y-directions. Magnetic field influence has been added to Navier–Stokes equations in Mramor, Vertnik, and Šarler (2014). They have used local collocation and multiquadratic RBFs on five-nodded subdomains and the coupling between pressure and velocity is made using fractional step method. Sellier, Aydın, and Tezer-Sezgin (2014) gives an analytical approach for solving 2D MHD Stokes flow produced by the rigid body motion of a solid particle.

Abbassi and Ben Nassrallah (2007) investigated the forced convection flow of a viscous incompressible electrically conducting fluid in a backward-facing step under an external magnetic field acting perpendicular to the channel (plane). In this case, increase in the strength of the magnetic field reduces the size of the flow in front of the step.

The use of local RBF collocation method was first presented by Vertnik and Šarler (2006), Šarler and Vertnik (2006) to diffusion problems and to diffusion–convection problems. Later, method is extended to solve natural convection problems by Kosec and Šarler (2008), and natural convection flow under a magnetic field by Mramor, Vertnik, and Šarler (2013). In these studies, it is indicated that local RBF takes less computational time compared to other numerical methods.

In this paper, MHD Stokes flow equations are formulated in terms of velocity components, pressure, stream function and vorticity which are all Poisson's type equations. Thus, the use of RBF collocation is carried simply with linear polynomial RBFs. The unknown pressure and vorticity boundary conditions are found from the momentum equations and vorticity definition with the help of coordinate matrix and finite difference approximations of derivatives. The present iterative scheme is validated with the solution of Stokes flow. The lid-driven cavity and backward-facing step flow problems are solved with horizontal, and horizontal and vertical external magnetic fields, respectively. The lid-driven cavity and backward-facing step flow results are given in Gürbüz and Tezer-Sezgin (2015a, 2015b) in the case of horizontal magnetic field. The main aim of this study was to show the effect of the external magnetic field on the Stokes flow behaviour in terms of all the original problem variables. In addition, the MHD flow in a lid-driven cavity, imposed to an external magnetic field acting in the pipe-axis direction which allows to generate electric potential in the flow, is solved for the first time to the best of author's knowledge. Thus, in this case, also electric potential is computed from a Poisson's equation as well as other flow field variables. Flow field, pressure and electric potential behaviours are presented in terms of equilines of the variables. Thus, the above-mentioned MHD Stokes flow benchmark problems are solved using simply linear polynomial approximation in RBF method. The RBF gives solution to MHD Stokes flow with considerably less computational expense compared to other numerical methods.

2. Physical problem (MHD Stokes flow)

We consider steady flow of a viscous, incompressible and electrically conducting fluid in channels under the influence of a uniform applied magnetic field. The governing coupled equations are the continuity equation, the Navier–Stokes equations of hydrodynamics and Maxwell's equations of electromagnetics through Ohm's law (Dragoş, 1975).

The motion of the fluid satisfies the equation of continuity (Yosinobu & Kakutani, 1959)

$$\nabla \cdot \mathbf{u} = 0 \tag{1}$$

and the momentum equations

$$\rho(\mathbf{u} \cdot \nabla)\mathbf{u} = -\nabla p + \rho\nu\nabla^2\mathbf{u} + \mathbf{J} \times \mathbf{B} \tag{2}$$

where $\mathbf{u}$, $\mathbf{B}$ and p are the velocity field, magnetic induction and pressure, respectively. ρ is the density, and ν is the kinematic viscosity. The electric field is $\mathbf{E} = -\nabla\phi$ where ϕ is the electric potential since $\nabla \times \mathbf{E} = 0$. From Ohm's law, the electric current density $\mathbf{J} = \frac{1}{\mu}\nabla \times \mathbf{B}$ is

$$\mathbf{J} = \sigma(\mathbf{E} + \mathbf{u} \times \mathbf{B}) \tag{3}$$

where σ and μ are the electric conductivity and magnetic permeability of the fluid. $\mathbf{J} \times \mathbf{B}$ is the Lorentz force and $\nabla \cdot \mathbf{B} = 0$ (magnetic induction is solenoidal). Now, we introduce the scaled transformations

$$\mathbf{x} \to \mathbf{x}L, \quad \mathbf{u} \to \mathbf{u}u_0, \quad \mathbf{H} \to \mathbf{H}H_0 \tag{4}$$

$$p \to p\rho\nu u_0/L, \quad \phi \to \phi\mu L u_0 H_0 \tag{5}$$

with $\mathbf{B} = \mu\mathbf{H}$ and substitute into Equations (1)–(3) to obtain the non-dimensional MHD equations as

$$\nabla \cdot \mathbf{u} = 0 \tag{6}$$

$$Re(\mathbf{u} \cdot \nabla)\mathbf{u} = -\nabla p + \nabla^2\mathbf{u} + M^2(-\nabla\phi + \mathbf{u} \times \mathbf{H}) \times \mathbf{H} \tag{7}$$

$$R_m(\mathbf{E} + \mathbf{u} \times \mathbf{H}) = \nabla \times \mathbf{H} \tag{8}$$

where $Re = Lu_0/\nu$, $R_m = Lu_0\sigma\mu$, and $M = L\mu H_0\sqrt{\sigma/\rho\nu}$ are the Reynolds number, the magnetic Reynolds number and the Hartmann number, respectively. $\mathbf{x}$, L and u_0 are the space variables, characteristic length and velocity. H_0 is externally applied magnetic field intensity. Taking negligible Re and R_m ($Re << 1, R_m << 1$), we obtain the 2D steady MHD Stokes equations

$$\nabla \cdot \mathbf{u} = 0 \tag{9}$$

$$-\nabla p + \nabla^2\mathbf{u} + M^2(-\nabla\phi \times \mathbf{H} + \mathbf{u} \times \mathbf{H} \times \mathbf{H}) = 0. \tag{10}$$

2.1. Horizontal or vertical external magnetic field

In the cross section of the channel, the flow is regarded as two-dimensional. When magnetic field applies horizontally Equations (9)–(10) can be written componentwise for $\mathbf{u} = (u, v, 0)$ and $\mathbf{H} = (H_0, 0, 0)$ as

$$\frac{\partial u}{\partial x} + \frac{\partial v}{\partial y} = 0 \tag{11}$$

$$\nabla^2 u = \frac{\partial p}{\partial x} \tag{12}$$

$$\nabla^2 v - M^2 v = \frac{\partial p}{\partial y}. \tag{13}$$

Introducing 2D stream function ψ to satisfy continuity equation and vorticity ω as $u = \dfrac{\partial \psi}{\partial y}$, $v = -\dfrac{\partial \psi}{\partial x}$ and $\omega = \dfrac{\partial v}{\partial x} - \dfrac{\partial u}{\partial y}$, we obtain stream function equation $\nabla^2 \psi = -\omega$. Differentiation of vorticity definition with respect to x and y and using continuity equation gives velocity–vorticity equations as

$$\nabla^2 u = -\frac{\partial \omega}{\partial y}, \quad \nabla^2 v = \frac{\partial \omega}{\partial x}. \tag{14}$$

Pressure Poisson's equation is obtained by differentiating Equations (12) and (13) with respect to x and y, respectively, and adding them up,

$$\nabla^2 p = -M^2 \frac{\partial v}{\partial y}. \tag{15}$$

Similarly, vorticity Poisson's equation can be derived from cross-differentiation of Equations (12) and (13) as

$$\nabla^2 \omega = M^2 \frac{\partial v}{\partial x}. \tag{16}$$

Thus, the two-dimensional MHD Stokes flow is represented with Poisson's type equations in terms of velocity components, stream function, vorticity and pressure

$$\nabla^2 u = -\frac{\partial \omega}{\partial y}, \quad \nabla^2 v = \frac{\partial \omega}{\partial x} \tag{17}$$

$$\nabla^2 \psi = -\omega \tag{18}$$

$$\nabla^2 \omega = M^2 \frac{\partial v}{\partial x}, \quad \nabla^2 p = -M^2 \frac{\partial v}{\partial y}. \tag{19}$$

When the magnetic field applies in the y-direction, $\mathbf{H} = (0, H_0, 0)$, Equations (9)–(10) take the form

$$\frac{\partial u}{\partial x} + \frac{\partial v}{\partial y} = 0 \tag{20}$$

$$\nabla^2 u - M^2 u = \frac{\partial p}{\partial x} \tag{21}$$

$$\nabla^2 v = \frac{\partial p}{\partial y} \tag{22}$$

which are put again into Poisson's equations for velocity components, stream function, vorticity and pressure

$$\nabla^2 u = -\frac{\partial \omega}{\partial y}, \quad \nabla^2 v = \frac{\partial \omega}{\partial x} \tag{23}$$

$$\nabla^2 \psi = -\omega \tag{24}$$

$$\nabla^2 \omega = -M^2 \frac{\partial u}{\partial y}, \quad \nabla^2 p = -M^2 \frac{\partial u}{\partial x}. \tag{25}$$

The difference is only in the right hand sides of vorticity and pressure Poisson's equations. Velocity and stream function equations are not affected with the direction of magnetic field.

2.2. Applied magnetic field in the z-direction

External magnetic field applying in the pipe-axis direction results in $\mathbf{H} = (0, 0, H_0)$ and momentum Equation (10) is affected from electric current density $\mathbf{J}$ as

$$\frac{\partial u}{\partial x} + \frac{\partial v}{\partial y} = 0 \tag{26}$$

$$\nabla^2 u = \frac{\partial p}{\partial x} - M^2 \left(-\frac{\partial \phi}{\partial y} - u \right) \tag{27}$$

$$\nabla^2 v = \frac{\partial p}{\partial y} - M^2 \left(\frac{\partial \phi}{\partial x} - v \right). \tag{28}$$

Since $\nabla \cdot \mathbf{J} = 0$, Ohm's law (3) gives electric potential equation as

$$\nabla^2 \phi = \omega. \tag{29}$$

This Poisson's equation results only for the case of magnetic field applied in the pipe-axis direction. For vertically or horizontally applied magnetic fields, this equation reduces to Laplace equation and with zero boundary conditions gives zero electric potential.

Now, the equations for pressure and vorticity by differentiating Equations (27)–(28) become Laplace equations too

$$\nabla^2 p = 0, \quad \nabla^2 \omega = 0. \tag{30}$$

Thus, MHD Stokes flow equations in terms of stream function, electrical potential, velocity components, vorticity and pressure are coupled with electric potential through vorticity in the flow

$$\nabla^2 u = -\frac{\partial \omega}{\partial y}, \quad \nabla^2 v = \frac{\partial \omega}{\partial x} \tag{31}$$

$$\nabla^2 \psi = -\omega, \quad \nabla^2 \phi = \omega \tag{32}$$

$$\nabla^2 \omega = 0, \quad \nabla^2 p = 0 \tag{33}$$

where pressure is affected from electric potential in obtaining its boundary conditions from Equations (27)–(28). Boundary conditions for vorticity are obtained from its definition. For electric potential, both insulated ($\frac{\partial \phi}{\partial n} = 0$) and conducting ($\phi = c$) wall conditions are considered.

Thus, Equations (17)–(19), (23)–(25) and (31)–(33) are going to be used for solving MHD Stokes flow for the cases of external magnetic field acting in the x-direction, y-direction and z-direction, respectively.

3. RBF application

In the RBF approximation method (Chen, Fan, & Wen, 2012) the inhomogeneity in a partial differential equation $Lu(x, y) = f(x, y)$ is approximated as

$$f(x, y) \simeq \sum_{j=1}^{n} a_j \varphi_j(r), \quad (x, y) \in \Omega \tag{34}$$

where $r = \sqrt{(x - x_j)^2 + (y - y_j)^2}$ is the Euclidean distance and n is the number of unknown coefficients, $\varphi_j(r)$'s are RBFs and boundary condition is given also as $Bu(x, y) = g(x, y)$. L and B are linear operators, f and g are known functions in a domain Ω with the boundary $\partial\Omega$.

Then, we can write the approximate solution $\hat{u}$ as

$$\hat{u}(x, y) = \sum_{j=1}^{n} a_j \Psi_j(r) \tag{35}$$

where $\{\Psi_j\}$ is obtained by back substitution through the differential equation $L\Psi_j(r) = \varphi_j(r)$. Forcing $\hat{u}$ to satisfy the boundary condition $Bu = g$, we get

$$\sum_{j=1}^{n} a_j B\Psi_j(r) = g(x, y), \quad (x, y) \in \partial\Omega. \tag{36}$$

The undetermined coefficients a_j in the approximation (35) are obtained using the collocation method. Taking N boundary points (x_k, y_k), $1 \leq k \leq N$ and L interior points (x_l, y_l), $N + 1 \leq l \leq N + L$, we have two linear systems

$$\sum_{j=1}^{n} a_j B\Psi_j(r_k) = g(x_k, y_k), \quad 1 \leq k \leq N \tag{37}$$

and

$$\sum_{j=1}^{n} a_j \varphi_j(r_l) = f(x_l, y_l), \quad 1 + N \leq l \leq n \tag{38}$$

where $n = N + L$. So, we combine the two systems to obtain a linear system

$$[A]\{a\} = \{b\} \tag{39}$$

for the solution vector $\{a\} = \begin{bmatrix} a_1 & \cdots & a_n \end{bmatrix}^t$ where the coefficient matrix and the right-hand side vector are given as

$$[A] = \begin{bmatrix} B\Psi_1(r_1) & B\Psi_2(r_1) & \cdots & B\Psi_n(r_1) \\ \vdots & \vdots & \ddots & \vdots \\ B\Psi_1(r_N) & B\Psi_2(r_N) & \cdots & B\Psi_n(r_N) \\ \varphi_1(r_{N+1}) & \varphi_2(r_{N+1}) & \cdots & \varphi_n(r_{N+1}) \\ \vdots & \vdots & \ddots & \vdots \\ \varphi_1(r_n) & \varphi_2(r_n) & \cdots & \varphi_n(r_n) \end{bmatrix}_{n\times n}, \{b\} = \begin{bmatrix} g(x_1, y_1) \\ \vdots \\ g(x_N, y_N) \\ f(x_{N+1}, y_{N+1}) \\ \vdots \\ f(x_n, y_n) \end{bmatrix}_{n\times 1}.$$

Solving the system (39) using Gaussian elimination, we get the coefficients a_j's, $1 \leq j \leq n$. Thus, the approximate solution $\hat{u}$ is obtained from

$$\hat{u}(x, y) = \sum_{j=1}^{n} a_j \Psi_j(r).$$

The coefficient matrix is full-matrix and does not show a special form. RBFs $\varphi_j(r)$ can be taken as polynomial, multiquadratics, conical RBFs, polyharmonic splines and the non-singular form of A must be carefully maintained with those choices.

3.1. Application to MHD Stokes flow equations with the x- or y- direction magnetic field

In this study, we take polynomial (linear) RBF $\varphi(r) = 1 + r$, and thus $\Psi(r) = \frac{r^2}{4} + \frac{r^3}{9}$. When the magnetic field is taken in the x-direction, MHD Stokes flow Equations (17)–(19) are Poisson's type equations. Thus, we solve all of them using RBF approximations iteratively. For the $u-$velocity equation we take $f = -\frac{\partial \omega}{\partial y}$ which can be computed using coordinate matrix F constructed from $f_{ij} = \varphi(r_{ij})$ as $f = -F_y F^{-1} w$ and $g = u_0$ is given with an initial estimate $\omega^{(0)}$. Similarly, the $v-$velocity equation is solved with $g = v_0$. Inhomogeneities in the stream function, vorticity and pressure equations are $-\omega$, $M^2 \frac{\partial v}{\partial x}$ and $-M^2 \frac{\partial v}{\partial y}$, respectively, and approximated similarly. Boundary values of pressure are derived using coordinate matrix F in Laplacian of u and v, and the finite difference

approximation for the pressure space derivatives in (12) and (13). Vorticity boundary values are either taken from vorticity definition $\omega = \frac{\partial v}{\partial x} - \frac{\partial u}{\partial y} = \frac{\partial F}{\partial x}F^{-1}v - \frac{\partial F}{\partial y}F^{-1}u$ using coordinate matrix F or finite difference approximation of $\nabla^2\psi = -\omega$ is used.

When magnetic field applies vertically, $\mathbf{H} = (0, 1, 0)$, we solve MHD slow flow Equations (23)–(25) using RBF approximation iteratively. For this case, we use the same procedure for velocity components and stream function. But, for solving vorticity equation we take $f = -M^2\frac{\partial u}{\partial y} = -M^2F_yF^{-1}u$ and the boundary values are obtained from the vorticity definition using the coordinate matrix. Pressure equation inhomogeneity is $f = -M^2\frac{\partial u}{\partial x} = -M^2F_xF^{-1}u$ and the boundary values are derived similarly as in the x-direction magnetic field case from Equations (21)–(22).

3.2. Application to MHD Stokes flow equations including electric potential

The steady slow flow of a viscous, incompressible and electrically conducting fluid under the influence of a uniform magnetic field in the z-direction is considered. The governing Equations (31)–(33) are solved using RBF approximation iteratively. The inhomogeneities are approximated using $\varphi(r) = 1 + r$ RBFs similarly as in the x-, y- direction magnetic field cases. For vorticity and pressure equations, the right-hand sides are zero, and the boundary values of ω and p are treated similarly with the F matrix and finite difference approximation of pressure derivatives.

4. Numerical results

The present iterative RBF approximation method has been applied to the Stokes flow under the influence of an applied uniform magnetic field either in the x-, y- or z-directions. In this study, two problems are considered: lid-driven square cavity flow under the effect of the x- or z-direction uniform magnetic field, backward-facing step flow in the presence of a horizontally and vertically applied uniform magnetic field. We solve MHD Stokes flow equations iteratively with a preassigned tolerance $\epsilon = 10^{-3}$ for the convergence. We use relaxation parameters α and β, $0 \leq \alpha, \beta \leq 1$ for vorticity and pressure, respectively, to accelerate the convergence.

4.1. Lid-driven cavity

The two-dimensional steady flow of a viscous, incompressible and electrically conducting fluid in a lid-driven rectangular cavity under the effect of a uniform horizontally applied magnetic field is considered. The Equations (17)–(19) are solved iteratively. The problem configuration and boundary values are shown in Figure 1.

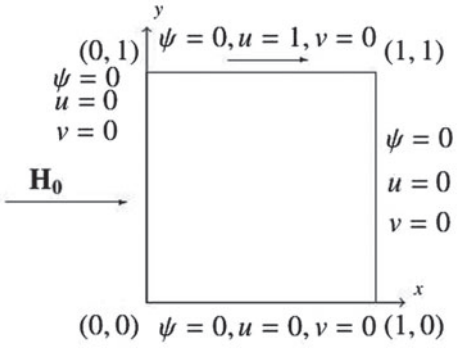

Figure 1. Lid-driven cavity.

The vorticity boundary conditions are obtained from the Equation (18) using the finite difference scheme which includes also interior ψ values. Thus, the boundary values for ω

$$\omega_0 = -\left(a_0\psi_0 + a_1\psi_p + a_2\psi_q + a_3\psi_n\Big|_0\right) \tag{40}$$

where ψ_0 is the boundary value, ψ_n is the normal derivative of ψ, ψ_p and ψ_q are interior values which are ph and qh distances away from the boundary and

$$a_0 = \frac{-2(p^3 - q^3)}{h^2p^2q^2(p-q)}, \qquad a_1 = \frac{-2q}{h^2p^2(p-q)}, \tag{41}$$

$$a_2 = \frac{2p}{h^2q^2(p-q)}, \qquad a_3 = \frac{-2(p+q)}{hpq}. \tag{42}$$

The pressure boundary values are obtained from the Equations (12)–(13) using coordinate matrix for the space derivatives and the finite difference scheme for the pressure gradients. Then, we have

$$p_b = p_i - \Delta y(Cv - M^2v) \quad \text{for the lower boundary} \tag{43}$$

$$p_b = p_i + \Delta xCu \quad \text{for the right boundary} \tag{44}$$

$$p_b = p_i + \Delta y(Cv - M^2v) \quad \text{for the upper boundary} \tag{45}$$

$$p_b = p_i - \Delta xCu \quad \text{for the left boundary} \tag{46}$$

where p_b is the boundary value, p_i is the interior value which is Δx or Δy distances away from the boundary and $C = \frac{\partial F}{\partial x}F^{-1}\frac{\partial F}{\partial x}F^{-1} + \frac{\partial F}{\partial y}F^{-1}\frac{\partial F}{\partial y}F^{-1}$ where F is the coordinate matrix constructed from $f_{ij} = 1 + r_{ij}$, r_{ij} being the distance between the points $'i'$ and $'j'$. We use relaxation parameters $\alpha = 0.01$ and $\beta = 0.001$ for vorticity and pressure, respectively. More boundary points N and interior points L are taken for increasing Hartmann number values. $60 \leq N \leq 140, 196 \leq L \leq 1156$ are taken for the range of M as $0 \leq M \leq 100$. Flow

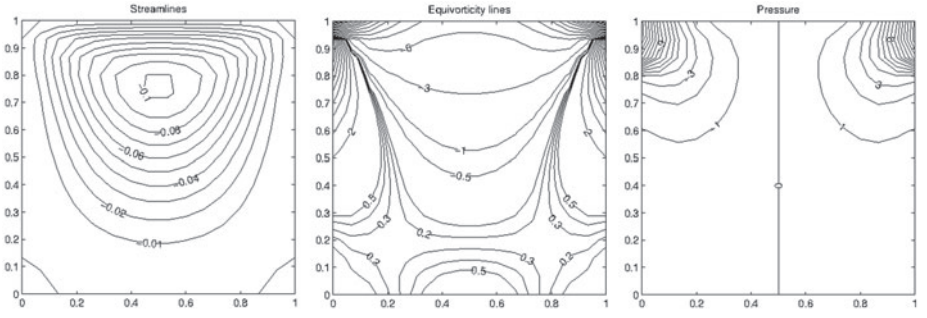

Figure 2. MHD Stokes flow for $M = 0$.

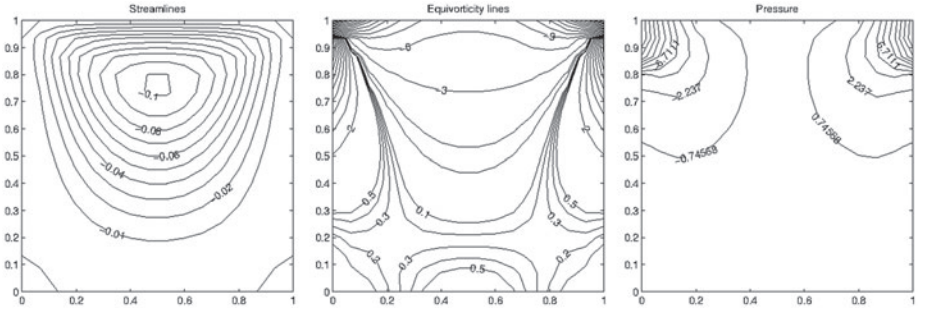

Figure 3. MHD Stokes flow for $M = 1$.

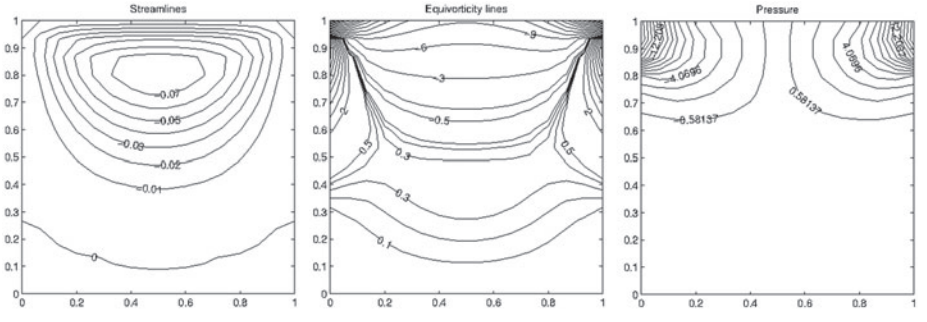

Figure 4. MHD Stokes flow for $M = 10$.

characteristics are shown in Figures 2–7 in terms of streamlines, equivorticity and pressure contours.

Figure 2 shows the flow symmetry with respect to vertical centreline which is expected in the Stokes flow, and streamlines, equivorticity and pressure lines are in well agreement with the ones in Young et al. (2006).

Figures 2–7 indicate that increasing the Hartmann number causes a decrease in the magnitude of stream function. Also, streamlines are getting closer to the moving boundary leaving the other part of the cavity with a secondary flow with small magnitude and later as stagnant region. A further increase in M

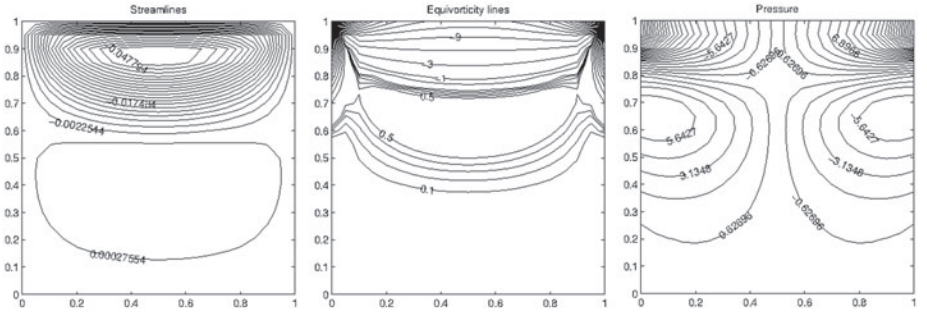

Figure 5. MHD Stokes flow for $M = 30$.

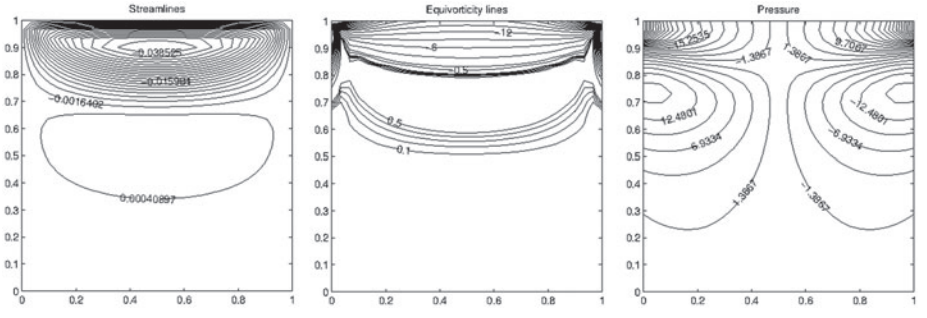

Figure 6. MHD Stokes flow for $M = 50$.

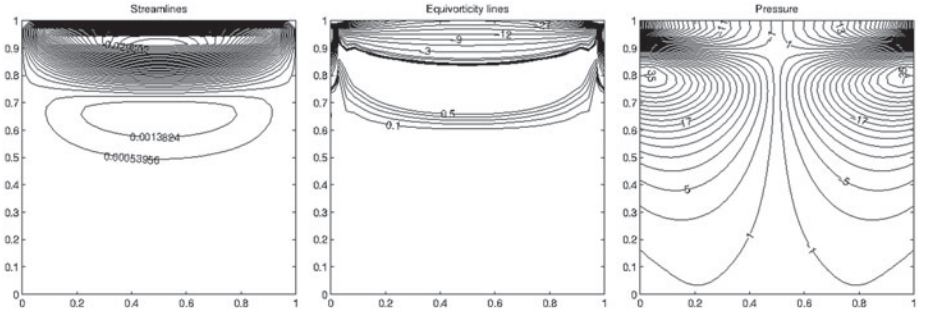

Figure 7. MHD Stokes flow for $M = 80$.

develops boundary layers in the direction of magnetic field (Hartmann layers) near the moving lid. These are the well-known characteristics of the MHD flow (flattening tendency of the flow and the boundary layer formation in the direction of applied magnetic field for increasing M). On the other hand, with an increase in the intensity of applied magnetic field vorticity profile is distorted appreciably. Boundary layer is developed towards moving boundary, and a secondary vortex starts to be seen just below the boundary layer. For $M \geq 30$ vorticity action is completely in front of the moving top lid in terms of two opposite direction bunch of vorticity lines. Again, rest of the cavity is stagnant. Moreover, when we

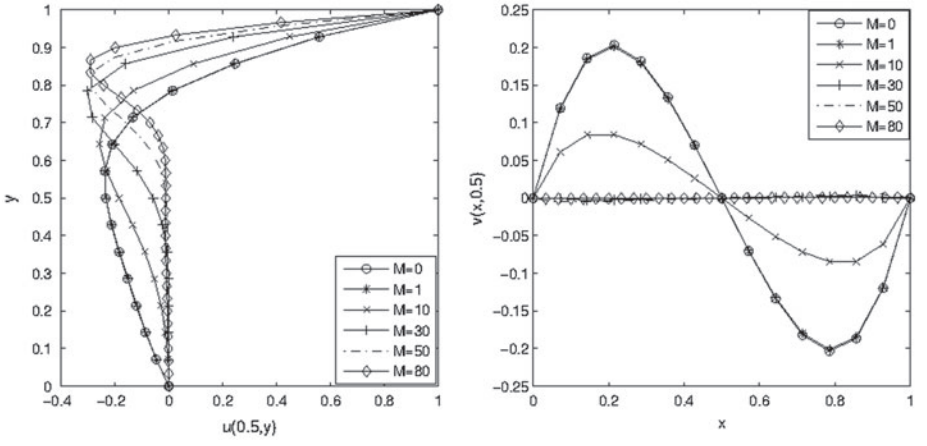

Figure 8. Centreline velocities.

look at the pressure profiles, we deduce that the increase in the intensity of the magnetic field increases pressure in the cavity. The moving lid also generates a pressure on the fluid close to the top. Thus, there are four antisymmetric vortices with respect to $x = 0.5$ line, two of them are separated from the others close to the moving lid. Hence, it may be regarded as a boundary layer in the separation region which is approximately $0.8 \leq y \leq 1.0$.

Figure 8 shows centreline velocity behaviours for increasing values of Hartmann number. The effect of applied magnetic field in x-direction is observed as the boundary layer formation near the moving lid. The well-known flattening tendency of MHD flow is observed from the decrease in magnitude of v as M increases. The centreline velocity profile for $M = 0$ (Stokes flow) is the same as the centreline velocities in Stokes flow obtained by Young et al. (2006). The efficiency of RBF is tested with dual reciprocity boundary element method (DRBEM) solution in terms of computational cost for $M = 0$ and $M = 30$ by taking the same number of boundary points as $N = 60$. It is seen that RBF requires nearly the half the computational time taken in DRBEM for obtaining solutions (Gürbüz and Tezer-Sezgin, 2015a).

4.2. Lid-driven cavity with electric potential

The steady slow flow of a viscous, incompressible and electrically conducting fluid is considered in a lid-driven square cavity under the influence of a uniform magnetic field in the z-direction. The Equations (31)–(33) are solved iteratively and the problem geometry with its wall conditions is shown in Figure 9. This problem differs from the Stokes flow only with the generation of electric potential due to the application of the magnetic field in the z-direction. Thus, the electric potential can be simulated. This problem is solved by taking potential boundary conditions as zero everywhere as well as considering top and bottom walls as conducting ($\phi = 0$) and vertical walls as insulated ($\frac{\partial \phi}{\partial n} = 0$).

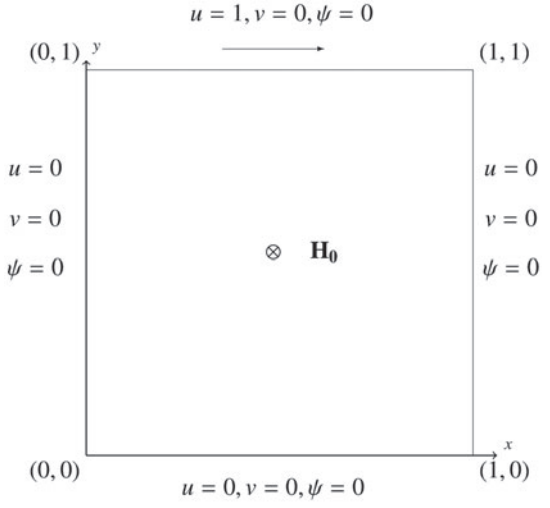

Figure 9. Lid-driven cavity with axis-direction magnetic field.

We use $N = 60, L = 196$. The flow characteristics are shown in Figures 10–11.

Figures 10–11 show the flow symmetry expected in the Stokes flow. Streamlines and electric equipotential lines have the same magnitude with opposite sign since $\nabla^2\phi = \omega$, $\nabla^2\psi = -\omega$. It is shown that the effect of magnetic field applied in the pipe-axis direction which enables to generate the electric potential with the interaction of electrically conducting fluid even in the Stokes flow. However, flow and pressure behaviours stay the same due to the Lorentz force terms cancelling each other in vorticity equation.

4.3. Backward-facing step channel Stokes flow

The iterative RBF approximation has been applied to the Stokes flow over backward-facing step under the effect of a horizontally or vertically applied uniform magnetic field. The problem configuration and boundary values are shown in Figure 12.

At the inlet, a parabolic velocity profile is prescribed. No-slip boundary conditions for u and v are imposed on the channel walls. At the exit, Neumann boundary conditions are imposed for u, w and ψ. Pressure reduces to zero and the y-velocity v is obviously zero at the exit.

4.3.1. Magnetic field in the x-direction

With a uniform magnetic field applied in the x-direction, MHD Stokes flow Equations (17)–(19) are solved iteratively using RBF approximation with relaxation parameters $\alpha = 0.01$, $\beta = 0.5$. At the inlet boundary, since a parabolic velocity profile is prescribed, the vorticity varies linearly and the fluid enters with a constant pressure. Unknown vorticity boundary conditions are obtained from the vorticity definition using the coordinate matrix F. The unknown pressure boundary values are obtained from Equations (12)–(13) using coordinate matrix

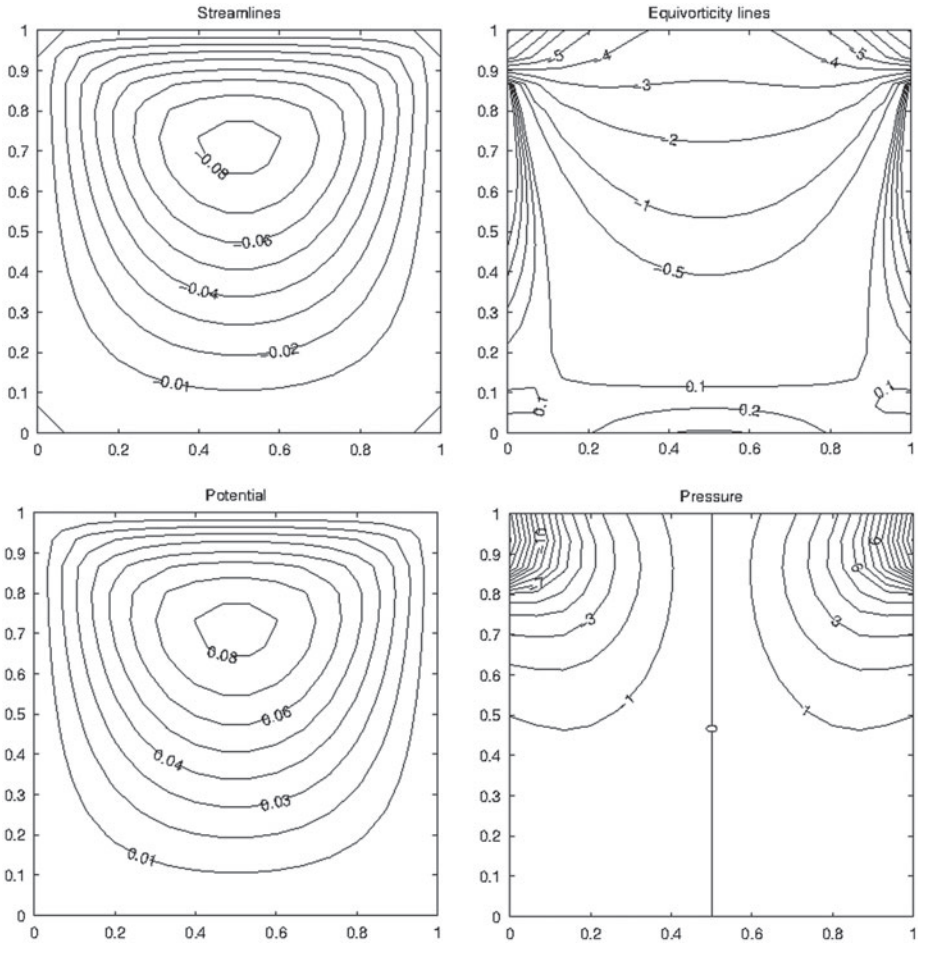

Figure 10. Stokes flow ($\phi|_{wall} = 0$).

F for the space derivatives and the finite difference scheme for the pressure gradients. Taking $N = 224$ (number of boundary points), $L = 1163$ (number of interior points) and the Hartmann number values as $M = 0, 10, 30, 90$, the flow characteristics are shown in Figures 13–17.

Figure 13 is in well agreement with the ones in Bustamante et al. (2013), since $M = 0$ for $Re << 1$ corresponds to the Stokes flow over a backward-facing step. Stream function starts the channel with a negative value. Effect of the step is small at $M = 0$ due to the slow motion of the fluid. In front of the step, the same direction recirculated flow appears (drops), but a secondary opposite direction flow is developed in the upper part of the channel starting around the step. Centreline velocities for $M = 0$ are presented in Figure 14 which are in well agreement with the Stokes step channel flow centreline velocities obtained by Bustamante et al. (2013).

As M increases with the effect of the x-direction magnetic field, as can be seen from Figures 15, 16 the recirculation flow in front of the step enlarges. The

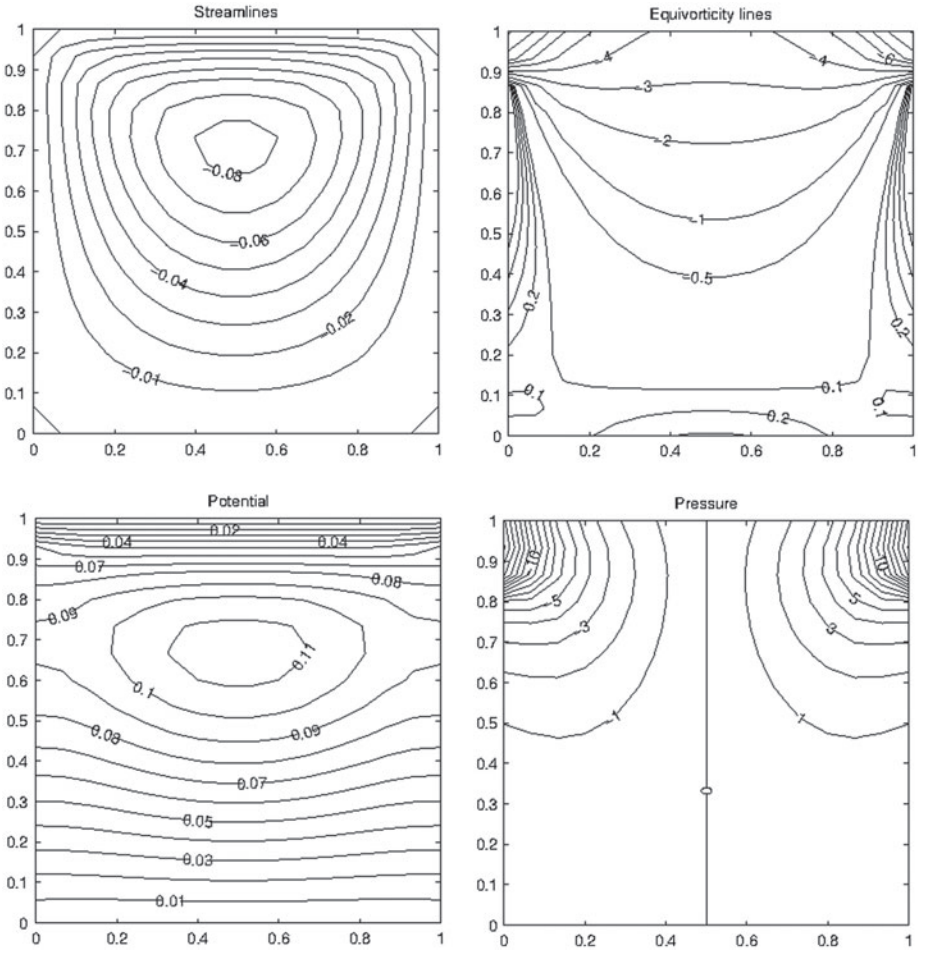

Figure 11. Stokes flow ($\frac{\partial \phi}{\partial n}|_{x=0,1}, \phi|_{y=0,1} = 0$).

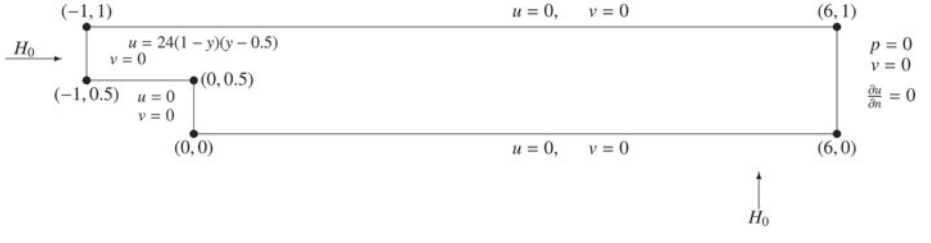

Figure 12. Backward-facing step flow.

secondary flow developed in front of the channel is squeezed through the upper wall and through the entrance. As M is increased further ($M = 90$), the same direction flow in front of the step which is small in magnitude tends to reach fully developed profile through the exit of the channel. This shows the effect of external magnetic field which is applied in the direction of the flow. The main

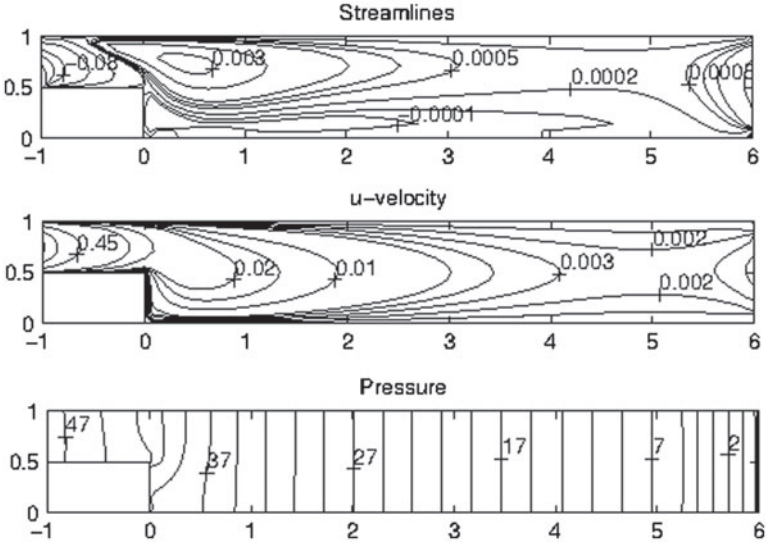

Figure 13. MHD Stokes flow for $M = 0$.

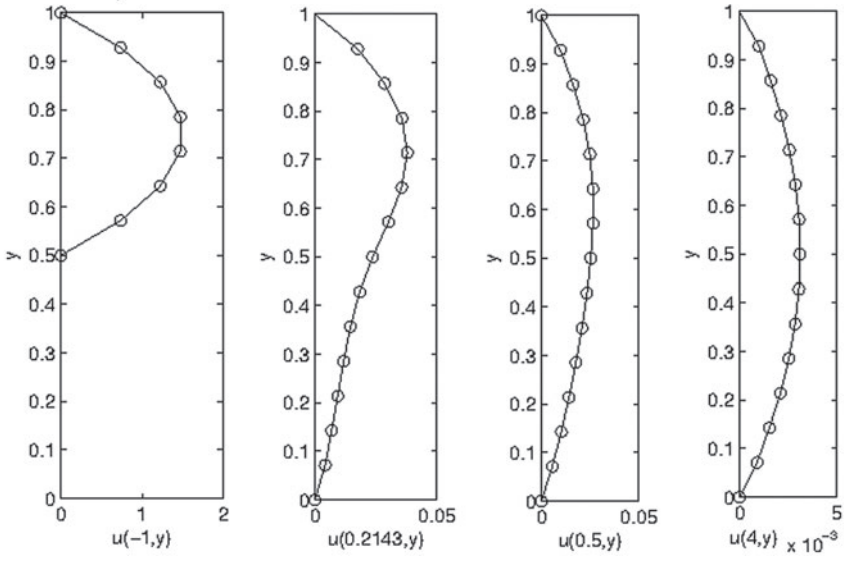

Figure 14. Centreline velocities for $M = 0$.

flow gets fully developed in a much shorter length of the channel as can be seen from Figure 17.

From the u-velocity figures, we also notice the drop of the fluid in front of the step from its parabolic profile. It reaches its fully developed profile through the exit. A further increase in M leaves a small stagnant region in front of the step and then overwhelms the effect of the step pushing the fluid above the bottom plate (Figure 17). Fluid enters the channel with a constant pressure, e.g. $p = 48$.

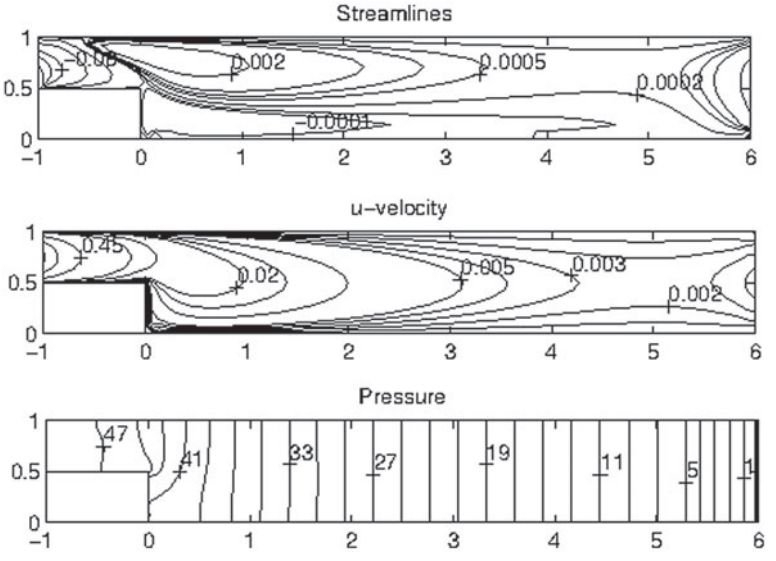

Figure 15. MHD Stokes flow for $M = 10$.

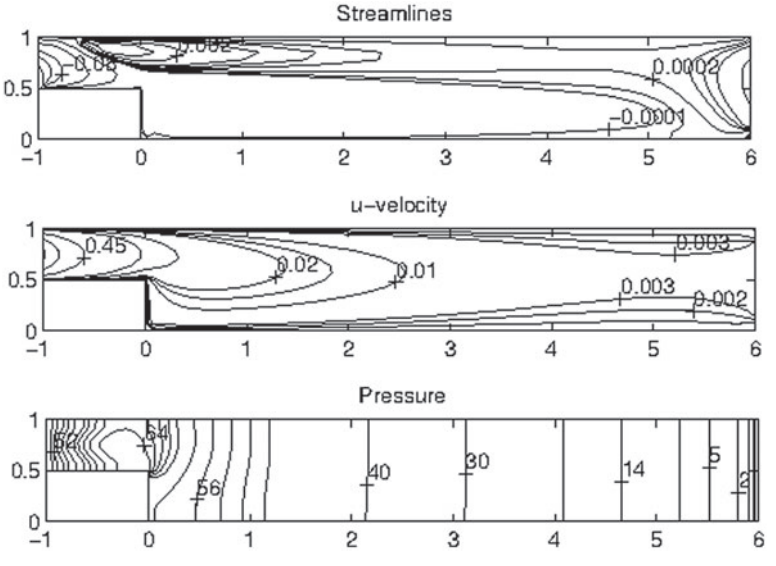

Figure 16. MHD Stokes flow for $M = 30$.

The step causes disturbance at the corner even at $M = 0$, and then, through the exit pressure diminishes smoothly ($p = 0$). Pressure of the fluid increases as M is increased, and the disturbance due to the step is more pronounced in the narrow entrance region and around the step with an increase in the intensity of the applied magnetic field. This is the expected behaviour of the pressure in a channel containing a step.

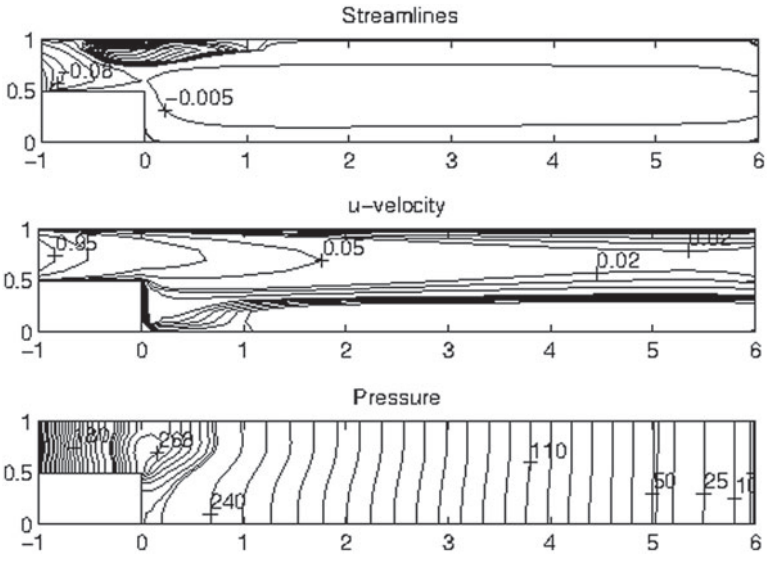

Figure 17. MHD Stokes flow for $M = 90$.

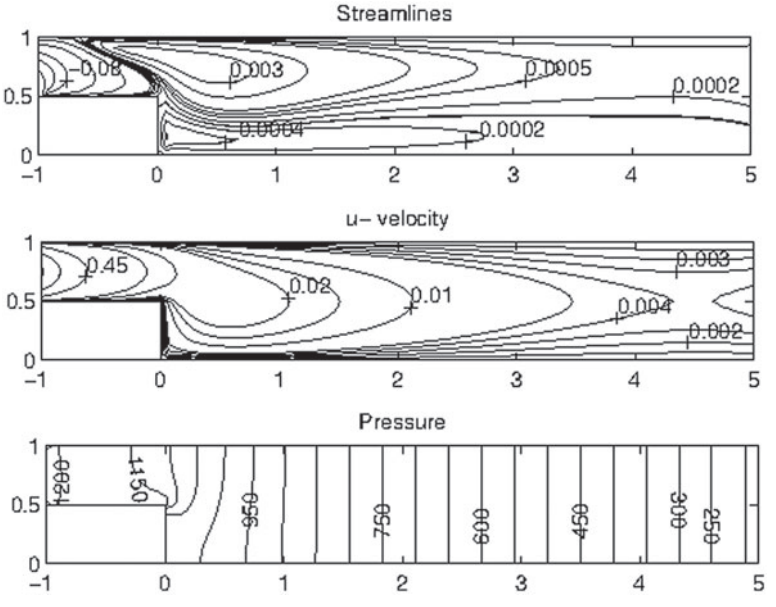

Figure 18. MHD Stokes flow for $M = 0$.

4.3.2. Magnetic field in the y-direction

RBF approximation has been applied to backward-facing step flow under the effect of vertical uniform magnetic field. Again, unknown vorticity and pressure boundary conditions are obtained from the vorticity definition using the coordinate matrix F, and from Equations (21)–(22) using coordinate matrix F for the space derivatives and the finite difference scheme for the pressure gradients,

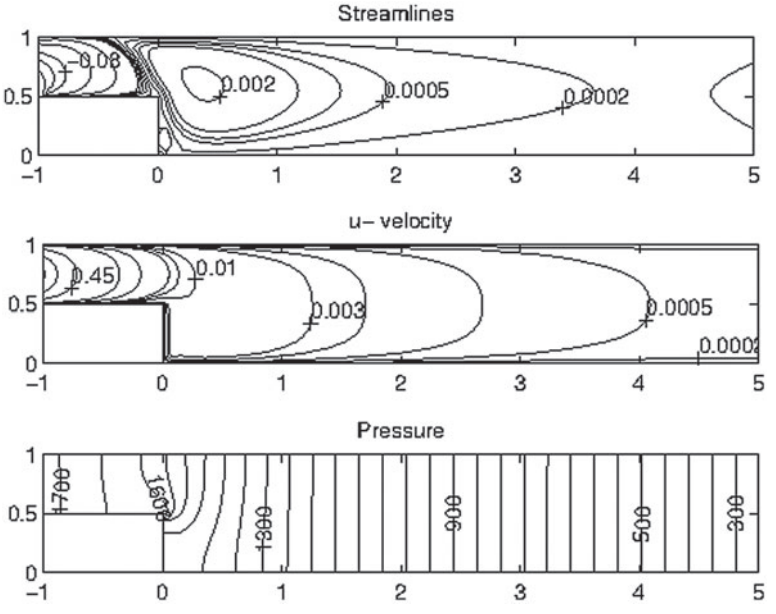

Figure 19. MHD Stokes flow for $M = 10$.

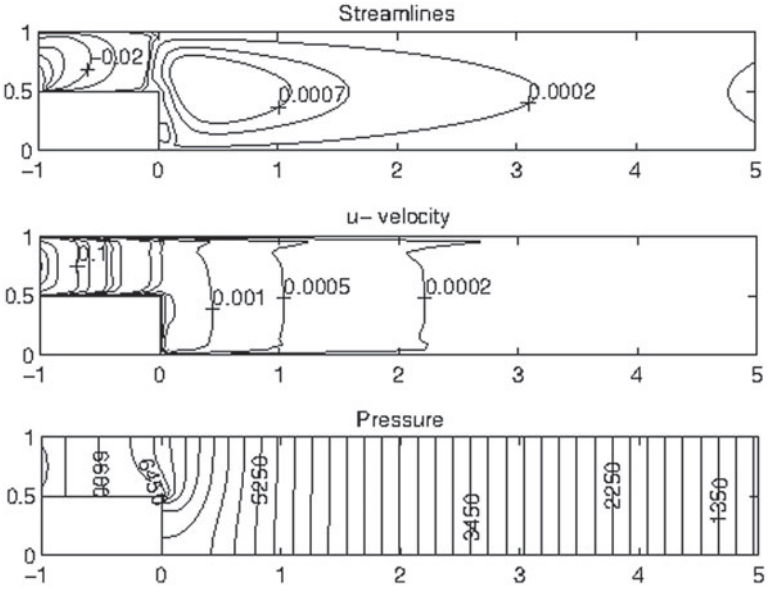

Figure 20. MHD Stokes flow for $M = 30$.

respectively. We solve MHD Equations (23)–(25) by taking $N = 200$, $L = 1463$ for $M = 0, 10, 30$ and $N = 224$, $L = 1649$ for $M = 50$. In Figure 18, we again present $M = 0$ case which is the Stokes flow as in Figure 13. The entrance (main) flow drops in front of the step, a secondary flow close to the upper plate extends through the channel. As M increases, secondary flow covers almost

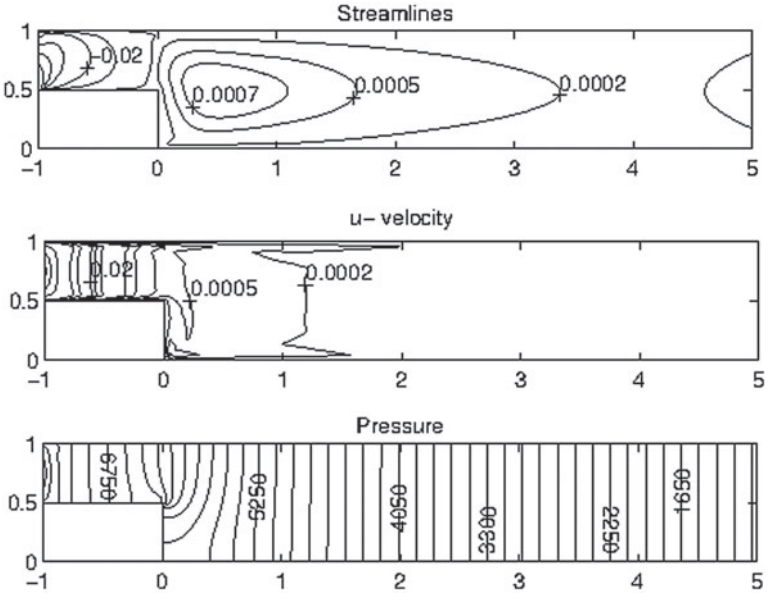

Figure 21. MHD Stokes flow for $M = 50$.

whole channel after the step. Meantime, main flow in front of the step is getting smaller as M gets larger, as can be seen from Figures 19–21. From the $u-$velocity profiles we deduce that as Hartmann number increases, fluid is pushed through the entrance and the flow is concentrated in front of the entrance region. Thus, the flow is retarded with decreasing magnitude throughout the channel.

The increase in the intensity of the magnetic field increases pressure magnitudes. For satisfying the exit condition ($p = 0$) we should extend the length of the channel.

Thus, we deduce that magnetic field which is in the direction of the flow helps to fluid to reach fully developed flow in a much shorter length in the channel containing a step. However, magnetic field acting vertically forces the flow to concentrate in front of the entrance. To satisfy exit pressure boundary condition, we should extend the length of the channel for both cases. The disturbances close to the exit in streamlines and u-velocity are due to the exit conditions abruptly.

5. Conclusions

In this study, we solve MHD Stokes flow equations using RBF approximation. RBF collocation method is easy to program compared to other numerical methods, and discretisation of the region and its boundary is done with arbitrarily located collocation points. The solution is obtained with considerably low-computational cost.

For the lid-driven cavity problem, the effect of applied magnetic field in the x-direction is observed as the boundary layer formation near the moving lid and the flow is flattened. This shows that, even in the slow MHD flow (Stokes

approximation) externally applied magnetic field has considerable effect on the flow and pressure behaviours. Magnetic field acting in the pipe-axis direction generates electric potential which has the same behaviour of the flow.

Applying magnetic field horizontally or vertically over the backward-facing step flow, we can conclude that magnetic field which is in the same direction of the flow helps the fluid flow to reach its fully developed form before the exit. Magnetic field acting vertically diminishes the vortex in front of the step and pushes the fluid through the entrance causing retarded flow.

Disclosure statement

No potential conflict of interest was reported by the authors.

Funding

This work was supported by the National PhD Fellowship Programme of The Scientific and Technological Research Council of Turkey (TÜBİTAK) [grant number 2211]; METU project [grant number BAP-01-01-2015-006].

References

Abbassi, H., & Ben Nassrallah, S. (2007). MHD flow and heat transfer in a backward-facing step. *International Communications in Heat and Mass Transfer, 34*, 231–237.

Alves, C. J. S., & Silvestre, A. L. (2004). Density results using Stokeslets and a method of fundamental solutions for the Stokes equations. *Engineering Analysis with Boundary Elements, 28*, 1245–1252.

Bustamante, C. A., Power, H., Sua, Y. H., & Florez, W. F. (2013). A global meshless collocation particular solution method (integrated radial basis function) for two-dimensional Stokes flow problems. *Applied Mathematical Modelling, 37*, 4538–4547.

Chen, C. S., Fan, C. M., & Wen, P. H. (2012). The method of approximate particular solutions for solving certain partial differential equations. *Numerical Methods for Partial Differential Equations, 28*, 506–522.

Chen, C. W., Young, D. L., Tsai, C. C., & Murugesan, K. (2005). The method of fundamental solutions for inverse 2D Stokes problems. *Computational Mechanics, 37*, 2–14.

Dragoş, L. (1975). *Magneto-fluid Dynamics*. England: Abacus Press.

Fan, C. M., & Young, D. L. (2002). Analysis of the 2D Stokes flows by the non-singular boundary integral equation method. *International Mathematical Journal, 2*, 1199–1215.

Gürbüz, M., & Tezer-Sezgin, M. (2015a). Lid-driven cavity and backward-facing step Stokes flow under an applied magnetic field. In *Proceedings of Tenth UK Conference on Boundary Integral Methods UKBIM*, (pp. 66–75), University of Brighton, Brighton.

Gürbüz, M., & Tezer-Sezgin, M. (2015b). Two-dimensional Stokes flow of an electrically conducting fluid in a channel under uniform magnetic field. In *Proceedings of Advances in Boundary Element & Meshless Techniques XVI*, (pp. 126–131), Valencia: BETEQ.

Kefayati, G. H. R., Gorji-Bandpy, M., Sajjadi, H., & Ganji, D. D. (2012). Lattice Boltzmann simulation of MHD mixed convection in a lid-driven square cavity with linearly heated wall. *Scientia Iranica, Transactions B: Mechanical Engineering, 19*, 1053–1065.

Kosec, G., & Šarler, B. (2008). Solution of thermo-fluid problems by collocation with local pressure correction. *International Journal of Numerical Methods for Heat and Fluid Flow, 18*, 868–882.

Kutanaei, S. S., Roshan, N., Vosoughi, A., Saghafi, S., Barari, A., & Soleimani, S. (2012). Numerical solution of Stokes flow in a circular cavity using mesh-free local RBF-DQ. *Engineering Analysis with Boundary Elements, 36*, 633–638.

Mramor, K., Vertnik, R., & Šarler, B. (2013). Simulation of natural convection influenced by magnetic field with explicit local radial basis function collocation method. *Computer Modeling in Engineering and Sciences, 92*, 327–352.

Mramor, K., Vertnik, R., & Šarler, B. (2014). Simulation of laminar backward facing step flow under magnetic field with explicit local radial basis function collocation method. *Engineering Analysis with Boundary Elements, 49*, 37–47.

Šarler, B., & Vertnik, R. (2006). Meshfree explicit local radial basis function collocation method for diffusion problems. *Computers and Mathematics with Applications, 51*, 1269–1282.

Sellier, A., Aydın, S. H., & Tezer-Sezgin, M. (2014). Free-space fundamental solution of a 2D steady slow viscous MHD flow. *Computer Modeling in Engineering and Sciences, 102*, 393–406.

Smyrlis, Y. S., & Karageorghis, A. (2003). Some aspects of the method of fundamental solutions for certain biharmonic problems. *Computer Modeling in Engineering and Sciences, 4*, 535–550.

Tsai, C. C., Young, D. L., & Cheng, A. H.-D. (2002). Meshless BEM for three-dimensional Stokes flows. *Computer Modeling in Engineering and Sciences, 3*, 117–128.

Vertnik, R., & Šarler, B. (2006). Meshless local radial basis function collocation method for convective-diffusive solid-liquid phase change problems. *International Journal of Numerical Methods for Heat and Fluid Flow, 16*, 617–640.

Yosinobu, H., & Kakutani, T. (1959). Two-dimensional Stokes flow of an electrically conducting fluid in a uniform magnetic field. *Journal of the Physical Society of Japan, 14*, 1433–1444.

Young, D. L., Chen, C. W., Fan, C. M., Murugesan, K., & Tsai, C. C. (2005). The method of fundamental solutions for Stokes flow in a rectangular cavity with cylinders. *European Journal of Mechanics B/Fluids, 24*, 703–716.

Young, D. L., Jane, S. J., Fan, C. M., Murugesan, K., & Tsai, C. C. (2006). The method of fundamental solutions for 2D and 3D Stokes problems. *Journal of Computational Physics, 211*, 1–8.

Young, D. L., Jane, S. C., Lin, C. Y., Chiu, C. L., & Chen, K. C. (2004). Solutions of 2D and 3D Stokes laws using multiquadratics method. *Engineering Analysis with Boundary Elements, 28*, 1233–1243.